



HAL
open science

Shadowgraph Analysis of Non-equilibrium Fluctuations for Measuring Transport Properties in Microgravity in the GRADFLEX Experiment

Fabrizio Croccolo, C. Giraudet, Henri Bataller, R. Cerbino, A. Vailati

► **To cite this version:**

Fabrizio Croccolo, C. Giraudet, Henri Bataller, R. Cerbino, A. Vailati. Shadowgraph Analysis of Non-equilibrium Fluctuations for Measuring Transport Properties in Microgravity in the GRADFLEX Experiment. *Microgravity Science and Technology*, 2016, 28 (4), pp.467-475. 10.1007/s12217-016-9501-1 . hal-01804394

HAL Id: hal-01804394

<https://hal.science/hal-01804394v1>

Submitted on 6 Feb 2020

HAL is a multi-disciplinary open access archive for the deposit and dissemination of scientific research documents, whether they are published or not. The documents may come from teaching and research institutions in France or abroad, or from public or private research centers.

L'archive ouverte pluridisciplinaire **HAL**, est destinée au dépôt et à la diffusion de documents scientifiques de niveau recherche, publiés ou non, émanant des établissements d'enseignement et de recherche français ou étrangers, des laboratoires publics ou privés.

1

2 Shadowgraph Analysis of Non-equilibrium Fluctuations 3 for Measuring Transport Properties in Microgravity 4 in the GRADFLEX Experiment

5 Fabrizio Croccolo^{1,2} · Cédric Giraudet^{1,5} · Henri Bataller¹ · Roberto Cerbino³ ·
6 Alberto Vailati⁴

7 Received: 29 January 2016 / Accepted: 11 April 2016
8 © Springer Science+Business Media Dordrecht 2016

9 **Abstract** In a fluid system driven out of equilibrium by
10 the presence of a gradient, fluctuations become long-ranged
11 and their intensity diverges at large spatial scales. This
12 divergence is prevented vertical confinement and, in a stable
13 configuration, by gravity. Gravity and confinement also affect
14 the dynamics of non-equilibrium fluctuations (NEFs). In
15 fact, small wavelength fluctuations decay diffusively, while
16 the decay of long wavelength ones is either dominated by
17 buoyancy or by confinement. In normal gravity, from the
18 analysis of the dynamics one can extract the diffusion coeffi-
19 cients as well as other transport properties. For example, in a
thermodiffusion experiment one can measure the Soret coef-

ficient. Under microgravity, the relaxation of fluctuations 20
occurs by diffusion only and this prevents the determination 21
of the Soret coefficient of a binary mixture from the study 22
of the dynamics. In this work we propose an innovative 23
self-referencing optical method for the determination of the 24
thermal diffusion ratio of a binary mixture that does not 25
require previous knowledge of the temperature difference 26
applied to the sample. The method relies on the determi- 27
nation of the ratio between the mean squared amplitude 28
of concentration and temperature fluctuations. We investi- 29
gate data from the GRADFLEX experiment, an experiment 30
flown onboard the Russian satellite FOTON M3 in 2007. 31
The investigated sample is a suspension of polystyrene poly- 32
mer chains (MW=9,100g/mol, concentration 1.8wt %) in 33
toluene, stressed by different temperature gradients. The use 34
of a quantitative shadowgraph technique allows to perform 35
measurements in the absence of delicate alignment and cal- 36
ibration procedures. The statics of the concentration and 37
temperature NEFs are obtained and their ratio is computed. 38
At large wave vectors the ratio becomes constant and is 39
shown to be proportional to the thermal diffusion ratio of 40
the sample. 41

This article belongs to the Topical Collection: Advances in Gravity-
related Phenomena in Biological, Chemical and Physical Systems
Guest Editors: Valentina Shevtsova, Ruth Hemmersbach

✉ Fabrizio Croccolo
fabrizio.croccolo@univ-pau.fr

¹ Laboratoire des Fluides Complexes et leurs Réservoirs,
UMR-5150, Université de Pau et des Pays de l'Adour,
1 Allée du Parc Montauray, Anglet, France

² Centre National d'Etudes Spatiales (CNES), Paris, France

³ Dipartimento di Biotecnologie Mediche e Medicina
Traslazionale, Università degli Studi di Milano,
Via F.lli Cervi 93, 20090, Segrate, Italy

⁴ Dipartimento di Fisica, Università degli Studi di Milano,
Via Celoria 16, 20133, Milano, Italy

⁵ Present address: Erlangen Graduate School in Advanced
Optical Technologies (SAOT) and Friedrich-Alexander-
Universität Erlangen-Nürnberg (FAU), Paul-Gordan-Straße 6,
D-91052, Erlangen, Germany

Keywords Thermodiffusion · Microgravity ·
Non-equilibrium fluctuations · Shadowgraph ·
Transport properties

Introduction

Non-equilibrium fluctuations (NEFs) are dramatically dif- 46
ferent from equilibrium ones (EFs), because of the coupling 47
of the driving gradient with spontaneous velocity fluctua- 48
tions (Ortiz de Zárate and Sengers 2006). This results in a

Q1

49 huge amplification of NEFs that is way more efficient for
 50 long wavelength fluctuations. Indeed, the intensity of NEFs
 51 exhibits a power-law divergence as $I(q) \propto q^{-4}$, $q = 2\pi/\lambda$
 52 being the fluctuation wave number inversely proportional
 53 to the wave length λ of the fluctuation. This divergence is
 54 prevented only by the effect of gravity (Segrè and Sengers
 55 1993; Vailati and Giglio 1998, 1997) and by the vertical con-
 56 finement determined by the final size of the sample (Ortiz de
 57 Zárate et al. 2006). These two reducing effects also impact
 58 the dynamics of NEFs. In a stable configuration, gravity
 59 accelerates very large fluctuations in moving them towards
 60 iso-dense layers (Croccolo et al. 2006, 2007), while con-
 61 finement acts in combination with gravity slowing down
 62 even larger fluctuations, as shown recently (Giraudet et al.
 63 2015). Recently, also simulations studies have pointed out
 64 the importance of NE fluctuations in diffusive processes
 65 (Donev et al. 2011; Balboa Usabiaga and et al. 2012; Donev
 66 et al. 2014; Delong et al. 2014).

67 The GRADFLEX experiment, flown in 2007 onboard
 68 the Russian satellite FOTON-M3, aimed at showing the
 69 full power-law divergence of the intensity of NEFs upon
 70 removal of the gravity force. This result was fully achieved
 71 both qualitatively, as can be appreciated from the published
 72 images (Vailati et al. 2011) and videos (ESA website), and
 73 quantitatively, as shown in the published papers (Vailati
 74 et al. 2011; Takacs and et al. 2011; Cerbino et al. 2015).

75 Many other space-based experiments have pointed out
 76 the importance of diffusive processes especially in micro-
 77 gravity conditions (De Lucas and et al. 1989; Snell and
 78 Helliwell 2005; Barmatz et al. 2007; Beysens 2014; Hegseth
 79 et al. 2014) Shevtsova;2012 (Shevtsova et al. 2011, 2014).

80 One interesting aspect of NEFs is that their analysis pro-
 81 vides direct access to the transport coefficients associated
 82 to the physical processes involved, like diffusion or ther-
 83 modiffusion (the so-called Soret effect). This peculiarity
 84 has been capitalized in the past for measuring fluid trans-
 85 port properties such as the mass diffusion and the Soret
 86 coefficients (Croccolo et al. 2012; Giraudet et al. 2014),
 87 but can be, in principle, further extended to other proper-
 88 ties such as thermal diffusivity or viscosity. In the cited
 89 papers fluid properties were obtained on ground by the
 90 analysis of the dynamics of concentration NEFs. More
 91 specifically, the evaluation of the time decay for different
 92 wave numbers by means of dynamic Shadowgraph allows
 93 getting the mass diffusion coefficient from the behavior
 94 of fluctuations at large wave vectors, where fluctuations
 95 are dominated by diffusion. At the same time, the Soret
 96 coefficient can be obtained by evaluating the experimen-
 97 tal solutal Rayleigh number $Ra_s = \beta g \nabla c L^4 / (\nu D)$ that is
 98 related to the wave number where time decay shows a dis-
 99 tinct maximum, marking the transition from a regime for
 100 relaxation of the fluctuations dominated by diffusion, to
 101 one dominated by buoyancy (Croccolo et al. 2007, 2012).

102 Here $\beta = (1/\rho) \cdot (\partial\rho/\partial c)$ is the solutal expansion coeffi-
 103 cient, ρ the fluid density, c the weight fraction concentration
 104 of the denser component of the mixture, g the gravitational
 105 acceleration, ∇c the amplitude of the concentration gradi-
 106 ent, L the vertical extension of the sample, ν the kinematic
 107 viscosity and D the mass diffusion coefficient. While the
 108 same approach can be used in the absence of gravity for
 109 measuring the mass diffusion coefficient, one cannot get the
 110 Soret coefficient because the maximum in the time decay
 111 disappears, as the solutal Rayleigh number Ra_s vanishes.

112 Here we propose an alternative procedure to obtain the
 113 value of the Soret coefficient in microgravity. Our procedure
 114 relies on the simultaneous determination of the intensity of
 115 the temperature and concentration NEFs and on the fact that
 116 solutal fluctuations are generated by a concentration gra-
 117 dient driven by the imposed temperature gradient through
 118 the Soret effect. The Soret coefficient S_T is proportional to
 119 the ratio between the concentration gradient and the applied
 120 temperature one:

$$\Delta c = -S_T c_o (1 - c_o) \Delta T, \tag{1}$$

121 where Δc is the concentration difference between the top
 122 and the bottom of the cell, c_o the equilibrium concentration
 123 of the denser component, ΔT the temperature difference
 124 between the top and the bottom of the cell. In this arti-
 125 cle we describe how to obtain a reliable measurement of
 126 the thermal diffusion ratio $k_T = T S_T c_o (1 - c_o)$, which is
 127 proportional to the Soret coefficient.

128 The remainder of the paper is organized as follows:
 129 Section “Theory and Methods” reports the theory and
 130 methods relevant to the analysis, in section “Results and
 131 Discussion” we provide results and discussion and in section
 132 “Conclusions” conclusions are drawn.

133 Theory and Methods

134 Thermodiffusion

135 When a thermal gradient is applied to a multi-component
 136 mixture, the different species undergo partial separation,
 137 which is contrasted by mass diffusion. The separation of
 138 the species is commonly named thermodiffusion or Soret
 139 effect (Soret 1879; de Groot and Mazur 1984). This sit-
 140 uation ends up at a steady state determined by a balance
 141 between Fickian diffusion and thermodiffusion when the
 142 corresponding fluxes are identical in the intensity and oppo-
 143 site in the direction, so that the total mass flux is zero
 144 $\vec{J} = \vec{J}_{Soret} + \vec{J}_{diffusion} = 0$. Imposing that the total mass
 145 flux is zero leads to Eq. 1, at steady state. The Soret effect
 146 can be thus conveniently utilized for generating a precisely

Q2

147 controllable and, in the case of small temperature differ-
 148 ences, linear concentration gradient in a fluid mixture by
 149 applying a temperature one.

150 **Non-Equilibrium Fluctuations**

151 The theory of non-equilibrium fluctuations has been ele-
 152 gantly described in the book by Ortiz de Zárate and Sen-
 153 gers (Ortiz de Zárate and Sengers 2006) and in references
 154 therein. Here we just would like to recall the main equations
 155 that will be used in the following. In particular we are inter-
 156 ested in a recent development of the theory that includes
 157 realistic boundary conditions in the case when gravity is
 158 removed (Ortiz de Zárate et al. 2015) the case relevant to
 159 the analysis of the GRADFLEX experiment. The assump-
 160 tion $g = 0$ led the authors derive an analytical solution for
 161 the dynamic structure factor of solutal NEFs :

$$S(\omega, q) = \frac{k_B T (\nabla c)^2}{\rho} \frac{2Dq^2}{\nu Dq^4 \omega^2 + D^2q^4} \left[1 + \frac{4(1 - \cosh \tilde{q})}{\tilde{q}(\tilde{q} + \sinh \tilde{q})} \right], \quad (2)$$

162 where k_B is the Boltzmann constant, T the average temper-
 163 ature, $\tilde{q} = qL$ the dimensionless wave number and L the
 164 vertical extension of the sample. This equation contains the
 165 main result that the dynamics of NEFs in microgravity show
 166 only diffusive behavior. Therefore the time constant can be
 167 expressed as a function of the wave number $\tau(q)$ as:

$$\tau(q) = \frac{1}{Dq^2}. \quad (3)$$

168 This behavior has been experimentally observed during
 169 the GRADFLEX experiment (Vailati et al. 2011; Cerbino
 170 et al. 2015).

171 For temperature fluctuations an exact theory including
 172 confinement effects is not available, but one can derive the
 173 exact expression of the intensity of NE fluctuations in the
 174 limit of large wave numbers (Ortiz de Zárate and Sengers
 175 2006)

$$\frac{S_{TT}^{NE\infty}}{S_{TT}^E} = \frac{c_p (\nabla T)^2}{T \alpha_T (\alpha_T + \nu)} L^4, \quad (4)$$

176 where c_p is the heat capacity at constant pressure, α_T the
 177 thermal diffusivity and:

$$S_{TT}^E = \frac{k_B T^2}{\rho c_p}, \quad (5)$$

178 is the intensity of the thermal fluctuations at equilibrium,
 179 independent of the wave number. For NE concentration
 180 fluctuations, by integrating Eq. 2 over the temporal fre-
 181 quencies and in the limit of large wave numbers, one gets:

$$S_{cc}^{NE\infty} = \frac{k_B T (\nabla c)^2}{\rho} \frac{1}{\nu D} L^4. \quad (6)$$

The ratio $S_{cc}^{NE\infty} / S_{TT}^{NE\infty}$ can thus be deduced from
 Eqs. 4–6:

$$\left(\frac{S_{cc}}{S_{TT}} \right)^{NE,\infty} = \frac{(\nabla c)^2 \alpha_T (\alpha_T + \nu)}{\nu D (\nabla T)^2}.$$

By including the definition of the Soret coefficient pro-
 vided by Eq. 1 one finally obtains:

$$\begin{aligned} \left(\frac{S_{cc}}{S_{TT}} \right)^{NE,\infty} &= \frac{\alpha_T (\alpha_T + \nu)}{\nu D} [c_0 (1 - c_0) S_T]^2 \\ &= \frac{\alpha_T (\alpha_T + \nu)}{\nu D} \frac{k_T^2}{T^2} \approx \frac{\alpha_T}{D} \frac{k_T^2}{T^2}. \end{aligned} \quad (7)$$

From Eq. 7 one can thus obtain k_T after measuring the
 ratio $S_{cc}^{NE\infty} / S_{TT}^{NE\infty}$ and knowing the two other quantities
 α_T and D . It's worth noting that only the amplitude of k_T
 can be retrieved with no information about its sign.

GRADFLEX Experiment

The GRADFLEX experiment (Vailati et al. 2006) was actu-
 ally composed of two distinct parts, one analyzing the
 behavior of temperature fluctuations in a simple fluid and
 another one analyzing solutal fluctuations in a binary mix-
 ture. Here we report and discuss only results from the latter
 experiment. The binary mixture under investigation is a
 colloidal suspension of polystyrene (PS) with a molecular
 weight of 9,100g/mol at a weak concentration of 1.8%w/w
 dissolved in pure toluene. The small concentration allows
 considering the limit of dilute sample and neglecting inter-
 actions between the polymer chains.

Experimental Procedures

The sample was confined by two 12-mm-thick sapphire
 windows placed at a distance of 1mm. The temperature
 of each window was controlled independently by using an
 annular Thermo Electric Device governed by a Proportional
 Integral Derivative (PID) servo loop. The sample was also
 laterally confined by a flat Viton gasket with an inner diam-
 eter of 25mm. The measurement of the temperature was
 performed immediately outside the sapphire plates in order
 to minimize the time delay to the temperature PID con-
 trollers, thus resulting in a very efficient temperature control
 with an RMS of about 10mK over 24 hours. Further details
 about the design of the apparatus can be found in literature
 (Vailati et al. 2006, 2011).

A series of experiments was performed consisting in the
 application of three temperature differences (nominally 5,
 10 and 20K) and awaiting the mass diffusion time needed

219 for the system to evolve to the stationary state $\tau_s =$
 220 $L^2/D = 5000s$.

221 During the steady state series of images were acquired
 222 with constant time delay of $\Delta t = 10s$.

223 **Optical Setup**

224 The optical technique utilized is that of quantitative
 225 Shadowgraph (Settles 2001; Trainoff and Cannell 2002;
 226 Crococolo and Brogioli 2011) that allows both imaging of
 227 what happens inside the cell as well as light scattering mea-
 228 surements by means of statistical analysis of the acquired
 229 images. The optical setup consisted of a super-luminous
 230 light emitting diode at a wavelength of $680\pm 10nm$ cou-
 231 pled to a mono-mode fiber. The diverging beam exiting the
 232 fiber is steered by a mirror and collimated by an achro-
 233 matic doublet lens. The collimated beam passes through the
 234 sample recording phase modulations due to fluctuations of
 235 the refractive index and then through a relay lens before
 236 impinging onto the CCD camera detector.

237 **Image Analysis**

238 Images have been analysed by means of two different
 239 approaches: the first one is the Differential Dynamic Algo-
 240 rithm that is able to extract the intermediate scattering
 241 function (ISF) by analysing differences of images with
 242 increasing time delay; the second one is Thermal Gradi-
 243 ent Analysis that we introduce here and that relies on the
 244 analysis of static power spectra for thermal gradients to
 245 retrieve the static signal of non-equilibrium fluctuations. In
 246 the following the two methods are described in more details.

247 **a) Differential Dynamic Algorithm**

248 The Differential Dynamic Algorithm has been introduced
 249 in 2006 for the analysis of Shadowgraph and Schlieren
 250 images during ground-based free diffusion experiments of
 251 isothermal binary mixtures (Crococolo et al. 2006, 2007).
 252 The principle has been further applied to other near field
 253 optical techniques (Cerbino and Trappe 2008; Cerbino and
 254 Vailati 2009; Giavazzi and Cerbino 2014).

255 The main idea is that of calculating the structure function
 256 of the fluctuations of the image intensity, which is calculated
 257 as (Crococolo et al. 2006):

$$C_m(\vec{q}, \Delta t) = \left\langle |I(\vec{q}, t + \Delta t) - I(\vec{q}, t)|^2 \right\rangle_t, \quad (8)$$

258 where $I(\vec{q}, t)$ is the image intensity upon 2D-spatial Fourier
 259 transform and Δt the varying temporal delay between con-
 260 sidered images.

261 This signal is further investigated for each available wave
 262 vector as a function of the time delay Δt between images by
 263 fitting through the following equation:

$$C_m(q, \Delta t) = 2(A_{DDA}(q)(1 - f(q, \Delta t)) + B_{DDA}(q)), \quad (9)$$

264 where $A(q) = S(q) \cdot T(q)$ represents the static power spec-
 265 trum as the product of the optical transfer function $T(q)$
 266 and the static power spectrum of the concentration fluctu-
 267 ations $S(q)$. $A_{DDA}(q)$ is thus the measured amplitude of
 268 the decaying signal: in our experimental conditions this is
 269 equivalent to the concentration fluctuations, because ther-
 270 mal ones decay too fast to be captured at the acquisition rate
 271 of the CCD camera. Here q represents the wave number,
 272 i.e. the amplitude of the wave vector \vec{q} after azimuthal aver-
 273 aging. Finally, $B_{DDA}(q)$ represents the background noise
 274 of the DDA analysis that includes also all the signals that
 275 decay faster than the acquisition delay time, like thermal
 276 fluctuations, as stated above (Cerbino et al. 2015).

277 From this kind of analysis one gets access to the Interme-
 278 diate Scattering Function (ISF) of the system. In many cases
 279 a single exponential decay is a realistic assumption for the
 280 ISF of NEFs, as will be discussed further in the next section,
 281 so one can assume:

$$f(q, \Delta t) = \exp\left[-\frac{\Delta t}{\tau(q)}\right]. \quad (10)$$

282 Fitting of Eqs. 9 and 10 can thus provide the value of
 283 the time decay of the fluctuations for every wave number
 284 q . In the case of a microgravity experiment recent theo-
 285 ries confirm the prediction of a pure diffusive behavior of
 286 concentration NE fluctuations, even in the presence of non-
 287 negligible confinement effects, so that the time decay is
 288 expected to be described by Eq. 3 (Ortiz de Zárate et al.
 289 2015). A fitting of the experimental data of $\tau(q)$ as a func-
 290 tion of the wave number can thus provide a quantitative
 291 measurement of the mass diffusion coefficient.

292 **b) Thermal Gradient Analysis**

293 As stated in the previous paragraph, one can get the static
 294 power spectrum of fluctuations $A(q)$ directly from the DDA
 295 analysis, but the efficiency of this procedure is limited when
 296 the intensity of fluctuations is very small or when the time
 297 decays become smaller than the time acquisition step of
 298 the CCD camera, like it is the case here for fluctuations of
 299 wave number larger than about $200cm^{-1}$. In this paper we
 300 introduce thus a different approach that takes into account
 301 simultaneously the results obtained for the three applied
 302 thermal gradients. From the acquired images one can get
 information about the static power spectrum of fluctuations

303 by directly measuring the quantity (Brogioli et al. 2000;
304 Trainoff and Cannell 2002):

$$S_m(\vec{q}) = \left\langle |I(\vec{q}, t) - I_0(\vec{q}, t)|^2 \right\rangle_t, \quad (11)$$

305 where $I_0(\vec{q}, t) = \langle I(\vec{q}, t) \rangle_t$ is the FFT of the background
306 image. The measured static power spectrum can also be
307 expressed as:

$$S_m(q) = A_{stat}(q) + B_{stat}(q), \quad (12)$$

308 where $A_{stat}(q) = S_{stat}(q) \cdot T(q)$ represents the measured
309 static power spectrum as the product of the optical trans-
310 fer function $T(q)$ and the static power spectrum of the NE
311 fluctuations $S_{stat}(q) = S_s(q) + S_t(q)$, including both tem-
312 perature and solutal ones. Contrary to the DDA analysis, the
313 TGA provides the statics of the signal so that it is indepen-
314 dent of the frame rate of the CCD camera, therefore both
315 the solutal and thermal signals are measured. $B_{stat}(q)$ here
316 represents the background noise of the ‘statics’ related to all
317 the sources of noise such as the CCD camera and the entire
318 electronic system. It’s worth pointing out that the inten-
319 sity of solutal fluctuations is expected to be much larger
320 than that of the temperature ones, as it will be shown in
321 the Discussion section. Therefore, we can assume that the
322 static signal is mostly determined by solutal fluctuations
323 $S_{stat}(q) \approx S_s(q)$. Theoretical models predict a quadratic
324 dependence of the structure factor from the temperature
325 difference (see Eqs. 4 and 6):

$$S_m(q, \Delta T) = a_{TGA}(q) \cdot \Delta T^2 + B_{TGA}(q). \quad (13)$$

326 Here the term $a_{TGA}(q)$ is a sort of normalized static
327 power spectrum that factors out the dependence from the
328 three different thermal gradients used in the actual GRAD-
329 FLEX experiment. Of course the amplitude $A_{TGA}(q)$ can
330 eventually be recovered for any temperature gradient by
331 calculating $A_{TGA}(q) = a_{TGA}(q) \cdot \Delta T^2$. Finally, the
332 background obtained by the TGA analysis would, in prin-
333 ciple, identify with the one mentioned in the static power
334 spectrum: $B_{stat}(q) = B_{TGA}(q)$.

335 **Results and Discussion**

336 In the following, we report results of the analysis of the
337 images obtained by the GRADFLEX mixture experiment.
338 The images acquired during the flight have been stored
339 on dedicated solid state disks that have been recovered
340 after the FOTON M3 satellite reentry. The raw data of
Shadowgraph images contain both measurements of the

optical background $I_0(\vec{q}, t) = \langle I(\vec{q}, t) \rangle_t$ not evolving in 341
time, and the fluctuating signal that is related to refractive 342
index fluctuations within the sample. In Fig. 1 we report 343
four false colors images of differences of images taken at 344
steady state at different delay times of 10, 100, 1000 and 345
10000s. 346

Clearly, the contrast of the images is steadily increas- 347
ing with the delay time. Also a sort of characteristic size is 348
somewhat recognizable within the images, which is a signa- 349
ture of the transfer function of the shadowgraph technique. 350
This can be further appreciated in Fig. 4 when the power 351
spectrum of differences of images is presented. 352

353 **Evaluation of the Mass Diffusion Coefficient by DDA**
354 **Analysis**

From shadowgraph images the structure function 355
 $C_m(q, \Delta t)$ has been calculated as per Eq. 8 for all the 356
wave numbers available in our optical setup. In Fig. 2, three 357
examples of structure functions are plotted against the time 358
delay between images for three different wave numbers. 359
The data points are normalized between 0 and 1 to facilitate 360
comparison. 361

The decay times of fluctuations are determined by fit- 362
ting the data at each wave number by means of Eqs. 9 and 363
10 with the three free parameters defined above: $A_{DDA}(q)$, 364
 $\tau(q)$ and $B_{DDA}(q)$. The resulting time decays are plot- 365
ted in Fig. 3 as a function of the wave number q . The data

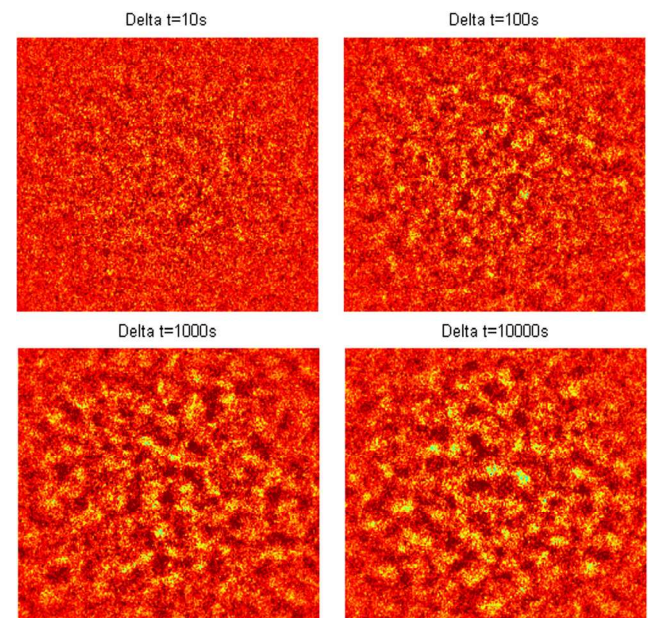


Fig. 1 False colors visualization of NE concentration fluctuations in microgravity. Data shown are for the maximum nominal temperature gradient at the steady-state of the thermodiffusion process. The side of each image is 13 mm

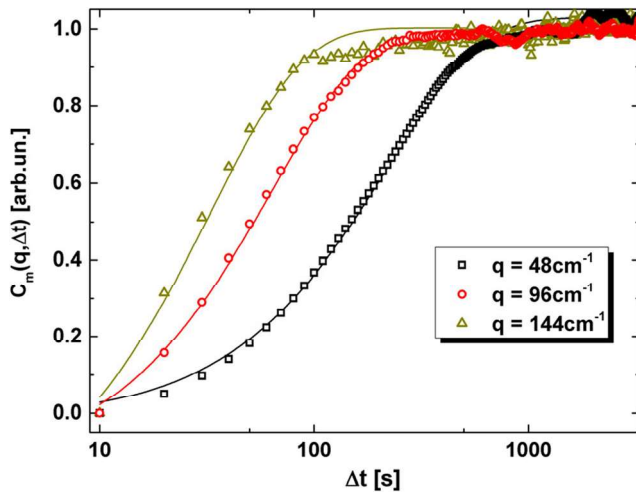


Fig. 2 Structure function $C_m(q, \Delta t)$ as a function of the time delay Δt for three different wave numbers q . Symbols stand for experimental data, while lines are the result of fitting with Eqs. 9 and 10

366 plotted in Fig. 3 represent the runs with nominal temperature
 367 difference of 20K, but equivalent results have been obtained
 368 for the other two temperature gradients.

369 The time decays in microgravity conditions should be
 370 well described by pure diffusive time constants mentioned
 371 above (Ortiz de Zárate et al. 2015), see Eq. 3. By fitting
 372 resulting time decays through Eq. 3 with the mass diffusion
 373 coefficient D as the only free parameter one gets the value
 374 $D = (2.03 \pm 0.04) \times 10^{-6} \text{ cm}^2/\text{s}$ in agreement with available
 375 data for the investigated mixture of PS in toluene (Vailati et
 376 al. 2011; Rauch and Kohler 2002, 2003).

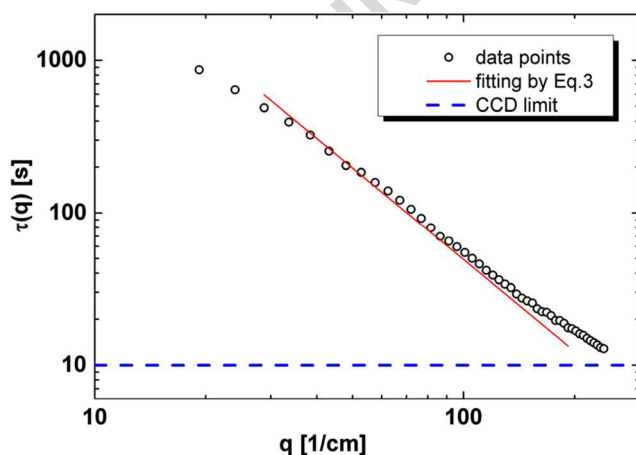


Fig. 3 Time decays $\tau(q)$ for the largest temperature gradient. The dashed blue line corresponds to the CCD delay time. The solid red line corresponds to the fitting with Eq. 3 using D as the only fitting parameter

Evaluation of the Statics by the TGA and Comparison with the DDA

377
 378

379 The static power spectrum $S_m(q)$ of NE fluctuations has
 380 also been evaluated by Eq. 11 for the three different temper-
 381 ature gradients applied in the GRADFLEX mixture exper-
 382 iment. Results are shown in Fig. 4. Note that the plot is
 383 in log-log scale and that the typical oscillations due to the
 384 Shadowgraph transfer function are clearly visible. The sig-
 385 nal is due to both solutal and thermal NE fluctuations,
 386 even if the solutal contribution is expected to be dominant.
 387 Here we also assume that the contribution of equilibrium
 388 fluctuations is contained into the background noise in the
 389 investigated range of wave numbers.

390 These data are then fitted through Eq. 13 for each wave
 391 number with $a_{TGA}(q)$ and $B_{TGA}(q)$ as free parameters.
 392 The values of the obtained background are plotted in Fig. 4
 393 for direct comparison to the signal. The oscillations typ-
 394 ical of the Shadowgraph technique are not present in the
 395 background signal.

396 The results for the quantity $A_{TGA}(q) = a_{TGA}(q) \cdot \Delta T^2$
 397 are shown in Fig. 5 calculated for the maximum thermal
 398 gradient together with the results of $A_{DDA}(q)$ obtained
 399 by means of the DDA algorithm. Clearly, the DDA algo-
 400 rithm fails in retrieving a satisfactory estimate of $A_{DDA}(q)$
 401 at wave numbers larger than about 200 cm^{-1} . It should be
 402 stressed again that the signal obtained by means of the
 403 analysis (black line in Fig. 5) is originated by concentra-
 404 tion fluctuations only, while the one obtained by the TGA
 405 analysis is the sum of the signal for solutal and thermal fluc-
 406 tuations. Actually in the DDA analysis and for the present
 407 experimental conditions, the signal of thermal fluctuations
 408 ends up in the background term $B_{DDA}(q)$ because its decay
 409 is too fast with respect to the image acquisition rate. Results

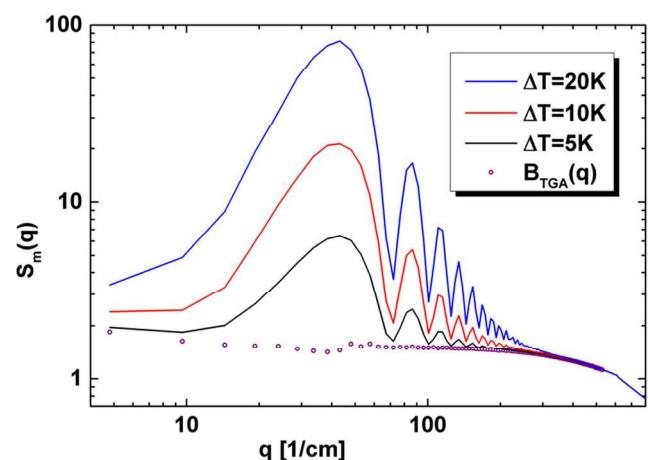


Fig. 4 Static power spectrum $S_m(q)$ for three temperature differences and the background resulting from fitting data through Eq. 13 as explained in the text

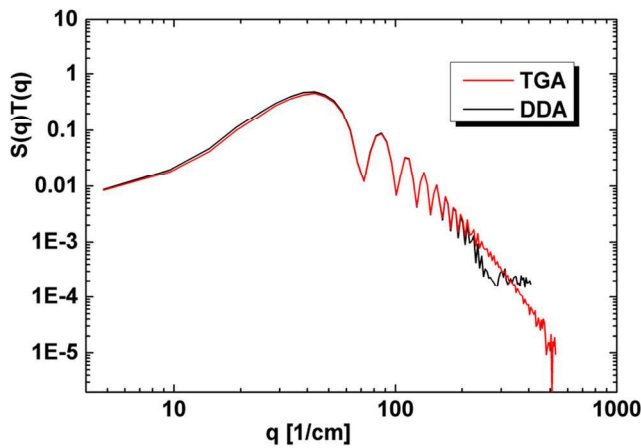


Fig. 5 Comparison between the quantity $A_{TGA}(q) = a_{TGA}(q) \cdot \Delta T^2$ obtained through the TGA analysis and $A_{DDA}(q)$ as obtained through the DDA one

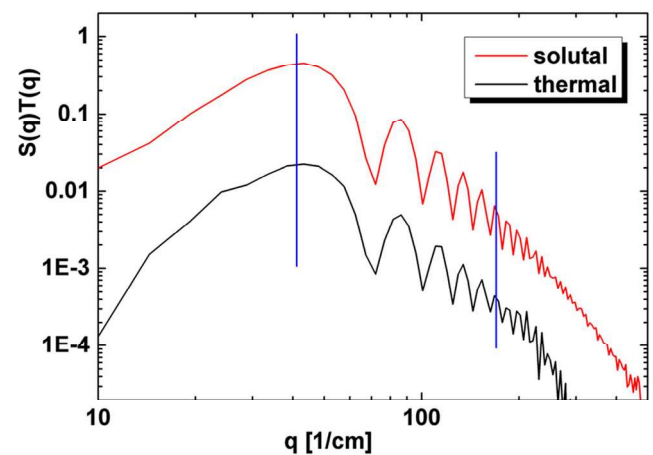


Fig. 7 Static power spectra for the solutal $A_{TGA}(q)$ and thermal $A_{therm}(q)$ NEFs

for $B_{DDA}(q)$ are shown in Fig. 6 for the three temperature differences.

By comparing Figs. 4 and 6 one can note that the intensity of thermal fluctuations is only roughly 5% of the total intensity, which justifies the assumption that solutal fluctuations are the main contribution of the signal. Therefore, we are now in the position of performing again the TGA analysis on the data of $B_{DDA}(q)$ shown in Fig. 6 in order to recover the static power spectrum of non-equilibrium thermal fluctuations only. We term the resulting parameter $a_{TGA,th}(q)$ to distinguish from the one previously obtained. The resulting $A_{therm}(q) = a_{TGA,th}(q) \cdot \Delta T^2$ is shown in Fig. 7 together with the result previously obtained for solutal fluctuations.

Again we stress that the intensity of the signal of thermal fluctuations is roughly one order of magnitude smaller

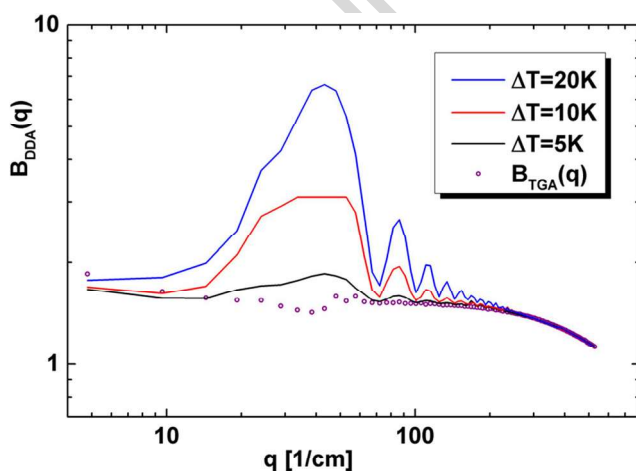


Fig. 6 DDA background $B_{DDA}(q)$ for the three temperature differences and the background resulting from fitting data through Eq. 13 as explained in the text

than that of solutal NEFs. Also we note that the quality of the signal for thermal fluctuations is worst because of the poorer signal to noise ratio. For thermal fluctuations data become almost unreliable outside the wave number range $40 \div 150 \text{ cm}^{-1}$. Vertical blue lines in Fig. 7 mark the mentioned range. To obtain further information about the static power spectrum of NEFs $S(q)$ one should divide the two signals shown in Fig. 7 by the shadowgraph transfer function $T(q)$, as done in (Vailati et al. 2011). This step requires a fine calibration of the optical technique, which introduces a number of undetermined sources of error. If one aims at retrieving the thermal diffusion ratio k_T , an alternative approach is that of calculating the ratio:

$$\frac{A_{TGA}(q)}{A_{therm}(q)} = \frac{S_{sol}(q) \cdot T(q)}{S_{th}(q) \cdot T(q)} = \frac{S_{sol}(q)}{S_{th}(q)}. \quad (14)$$

We recall that in the limit of large wave vectors this ratio should be equal to the result obtained in Eq. 7. One can further perform a fitting of the obtained data points in the wave number range around 100 cm^{-1} using k_T as fitting parameter in order to get an estimate of its value.

In Fig. 8 results of the ratio provided by Eq. 14 are shown as blue circle open symbols together with the theoretical prediction as a red continuous line and with the fitted value for large wave numbers. The theoretical curve is provided by the ratio of the theoretical predictions reported in Fig. 3 of (Cerbino et al. 2015), where the concentration intensity comes from a recent paper (Ortiz de Zárate et al. 2015) and the thermal one can be retrieved from the classical book (Ortiz de Zárate and Sengers 2006). The resulting value for the ratio is about 14 that results in a thermal diffusion ratio of $k_T = (1.0 \pm 0.2) \times 10^{-3} \text{ K}^{-1}$, in agreement with literature (Vailati et al. 2011; Rauch and Kohler 2002, 2003). We stress out here that the ratios provided by Eqs. 7 and 14 do not depend from the applied temperature

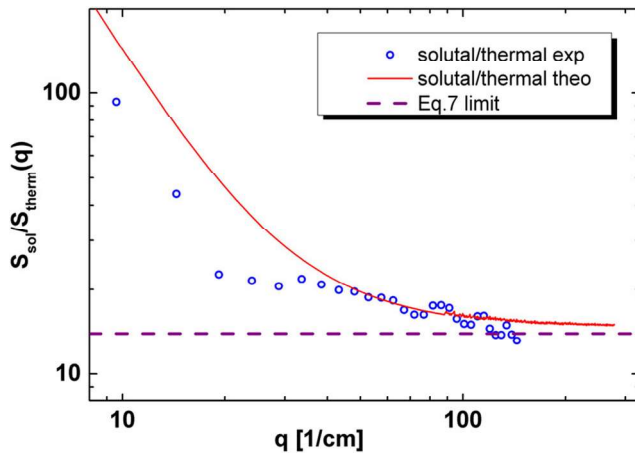


Fig. 8 Ratio of the static signal for solutal and thermal fluctuations. The dashed line represents the asymptotic value at large wave vectors

457 difference. Therefore, the procedure for the determination
 458 of the thermal diffusion ratio described here relies on a power-
 459 ful self-referencing method that works flawlessly even in
 460 the absence of the knowledge of the temperature gradient
 461 imposed to the sample. Moreover, the shadowgraph technique
 462 used by the method does not require any delicate
 463 optical alignment. These two features make the method proposed
 464 here a rugged solution ideal for the determination of
 465 transport coefficients under harsh conditions or in hostile
 466 environments.

467 Conclusions

468 In this paper we provide a further analysis of the images
 469 acquired during the GRADFLEX experiment in order to
 470 quantitatively measure the mass diffusion coefficient and
 471 the thermal diffusion ratio of a binary mixture of PS in
 472 toluene at weak concentration. These results confirm quantitatively
 473 the fact that the analysis of NE fluctuations can be efficiently
 474 performed by means of light scattering techniques like the shadowgraph
 475 able to detect wave numbers as small as 10/cm, thus getting access
 476 to the physical phenomena involved in the thermodiffusion process
 477 and providing a sound measurement of transport properties of the system.

478 Different image analysis procedures have been applied
 479 confirming previously published data. In particular a simple self-referencing
 480 method is proposed to measure both the mass diffusion coefficient
 481 and the thermal diffusion ratio. Remarkably, the method proposed
 482 by us does not require performing optical and thermal calibrations.
 483
 484

485 **Acknowledgments** We warmly thank D.S. Cannell, M. Giglio, S.
 Mazzoni, C.J. Takacs, O. Minster, A. Verga, F. Molster, N. Melville,

W. Meyer, A. Smart, R. Greger, B. Hirtz, and R. Pereira for their
 contribution to the GRADFLEX project. We gratefully acknowledge
 the European Space Agency (ESA) and the National Aeronautics and
 Space Administration (NASA) for support to ground-based activities.
 ESA is also thanked for sponsoring the flight opportunity. We
 acknowledge the contribution of the Telesupport team and of the industrial
 consortium led by RUAG aerospace. F.C. and H.B. acknowledge support
 from the French Centre Nationale d'Etudes Spatiales (CNES).

References

Balboa Usabiaga, F., et al.: Staggered schemes for fluctuating hydrodynamics. *SIAM J. Multiscale Model. Simul.* **10**, 1369–1408 (2012)

Barmatz, M., Hahn, I., Lipa, J.A., Duncan, R.V.: Critical phenomena in microgravity: past, present and future. *Rev. Mod. Phys.* **79**, 1–52 (2007)

Beysens, D.: Critical point in space: a quest for universality. *Microgravity Sci Tec.* **26**, 201–218 (2014)

Brogiooli, D., Vailati, A., Giglio, M.: Universal behavior of nonequilibrium fluctuations in free diffusion processes. *Phys. Rev. E* **61**, R1 (2000)

Cerbino, R., Trappe, V.: Differential dynamic microscopy: probing wave vector dependent dynamics with a microscope. *Phys. Rev. Lett.* **100**, 188102 (2008)

Cerbino, R., Vailati, A.: Near-field scattering techniques: Novel instrumentation and results from time and spatially resolved investigations of soft matter systems. *Curr. Opin. Colloid Interface Sci.* **14**, 416 (2009)

Cerbino, R., Sun, Y., Donev, A., Vailati, A.: Dynamic scaling for the growth of non-equilibrium fluctuations during thermophoretic diffusion in microgravity. *Sci. Rep.* **5**, 14486 (2015)

Crocco, F., Brogioli, D., Vailati, A., Giglio, M., Cannell, D.S.: Use of dynamic schlieren interferometry to study fluctuations during free diffusion. *App. Opt.* **45**, 2166 (2006)

Crocco, F., Brogioli, D., Vailati, A., Giglio, M., Cannell, D.S.: Non-diffusive decay of gradient-driven fluctuations in a free-diffusion process. *Phys. Rev. E* **76**, 041112 (2007)

Crocco, F., Batailler, H., Scheffold, F.: A light scattering study of non equilibrium fluctuations in liquid mixtures to measure the Soret and mass diffusion coefficient. *J. Chem. Phys.* **137**, 234202 (2012)

Crocco, F., Brogioli, D.: Quantitative Fourier analysis of schlieren masks: the transition from shadowgraph to schlieren. *App. Opt.* **50**, 3419 (2011)

de Groot, S.R., Mazur, P.: *Nonequilibrium Thermodynamics*. Dover, New York (1984)

Delong, S., Sun, Y., Griffith, B.E., Vanden-Eijnden, E., Donev, A.: Multiscale temporal integrators for fluctuating hydrodynamics. *Phys. Rev. E* **90**, 063312 (2014)

De Lucas, L.J., et al.: Protein crystal growth in microgravity. *Science* **246**, 651–654 (1989)

Donev, A., de la Fuente, A., Bell, J.B., Garcia, A.L.: Diffusive transport enhanced by thermal velocity fluctuations. *Phys. Rev. Lett.* **106**, 204501 (2011)

Donev, A., Fai, T.G., Vanden-Eijnden, E.: A reversible mesoscopic model of diffusion in liquids: from giant fluctuations to Fick's law. *J. Stat. Mech.* **P04004**, 1–39 (2014)

Giavazzi, F., Cerbino, R.: Digital Fourier microscopy for soft matter dynamics. *J. Opt.* **16**, 083001 (2014)

Giraudet, C., Batailler, H., Crocco, F.: High-pressure mass transport properties measured by dynamic near-field scattering of non-equilibrium fluctuations. *Eur. Phys. J. E* **37**, 107 (2014)

- 547 Giraudet, C., Bataller, H., Sun, Y., Donev, A., Ortiz de Zarate,
548 J.M., Croccolo, F.: Slowing-down of non-equilibrium concen-
549 tration fluctuations in confinement. *Europhys. Lett.* **111**, 60013
550 (2015)
- 551 Hegseth, J.J., Oprisan, A., Garrabos, Y., Beysens, D.: Imaging critical
552 fluctuations of pure fluids and binary mixtures. *Phys. Rev. E* **90**,
553 022127 (2014)
- 554 [http://www.esa.int/spaceinvideos/Videos/2011/06/
555 HugefluctuationsinGradflexexperiment](http://www.esa.int/spaceinvideos/Videos/2011/06/HugefluctuationsinGradflexexperiment)
- 556 Ortiz de Zárate, J.M., Sengers, J.V.: *Hydrodynamic Fluctuations*.
557 Elsevier, Amsterdam (2006)
- 558 Ortiz de Zárate, J.M., Fornés, J.A., Sengers, J.V.: Long-wavelength
559 nonequilibrium concentration fluctuations induced by the Soret
560 effect. *Phys. Rev. E* **74**, 046305 (2006)
- 561 Ortiz de Zárate, J.M., Kirkpatrick, T.R., Sengers, J.V.: Non-
562 equilibrium concentration fluctuations in binary liquids with real-
563 istic boundary conditions. *Eur. Phys. J. E* **38**, 99 (2015)
- 564 Rauch, J., Köhler, W.: Diffusion and thermal diffusion of semidi-
565 lute to concentrated solutions of polystyrene in toluene in the
566 vicinity of the glass transition. *phys. Rev. Lett.* **88**, 185901
567 (2002)
- 568 Rauch, J., Köhler, W.: Collective and thermal diffusion in dilute,
569 semidilute, and concentrated solutions of polystyrene in toluene.
570 *J. Chem. Phys.* **119**, 11977 (2003)
- 571 Segrè, P.N., Sengers, J.V.: Nonequilibrium fluctuations in liquid
572 mixtures under the influence of gravity. *Physica A* **198**, 46
573 (1993)
- 574 Settles, G.S.: *Schlieren and Shadowgraph Techniques*. Springer, Berlin
575 (2001)
- 576 Shevtsova, V.: IVIDIL experiment onboard the ISS. *Adv. Space Res.* **576 Q3**
577 **672**, 46–51 (2010)
- 578 Shevtsova, V., et al.: IVIDIL Experiment onboard ISS: thermodiffu-
579 sion in presence of controlled vibrations. *C. R. Mécanique* **339**,
580 310–317 (2011)
- 581 Shevtsova, V., et al.: Diffusion and soret in ternary mixtures. prepara-
582 tion of the DCMIX2 experiment on the ISS. *Microgravity Sci.*
583 *Technol.* **25**, 275–283 (2014)
- 584 Snell, E.H., Helliwell, J.R.: Macromolecular crystallization in micro-
585 gravity. *Rep. Prog. Phys.* **68**, 799–853 (2005)
- 586 Soret, C.: Etat d'équilibre des dissolutions dont deux parties sont
587 portées à des températures différentes. *Arch. Sci. Phys. Nat.* **3**, 48
588 (1879)
- 589 Takacs, C.J., et al.: Thermal fluctuations in a layer of CS₂ subjected
590 to temperature gradients with and without the influence of gravity.
591 *Phys. Rev. Lett.* **106**, 244502 (2011)
- 592 Trainoff, S., Cannell, D.S.: Physical optics treatment of the shadow-
593 graph. *Phys. Fluids* **14**, 1340 (2002)
- 594 Vailati, A., Giglio, M.: Giant fluctuations in a free diffusion process.
595 *Nature* **390**, 262 (1997)
- 596 Vailati, A., Giglio, M.: Nonequilibrium fluctuations in time-dependent
597 diffusion processes. *Phys. Rev. E* **58**, 4361 (1998)
- 598 Vailati, A., Cerbino, R., Mazzoni, S., Giglio, M., Nikolaenko, G.,
599 Takacs, C.J., Cannell, D.S., Meyer, W.V., Smart, A.E.: Gradient-
600 driven fluctuations experiment: fluid fluctuations in microgravity.
601 *App. Opt.* **45**, 2155 (2006)
- 602 Vailati, A., Cerbino, R., Mazzoni, S., Takacs, C.J., Cannell, D.S.,
603 Giglio, M.: Fractal fronts of diffusion in microgravity. *Nature*
604 *Comm.* **2**, 290 (2011)

UNCORRECTED